



## Structure of molten Al and eutectic Al–Si alloy studied by neutron diffraction

U. Dahlborg <sup>a</sup>, M.J. Kramer <sup>b</sup>, M. Besser <sup>b</sup>, J.R. Morris <sup>c</sup>, M. Calvo-Dahlborg <sup>a,\*</sup>

<sup>a</sup> GPM, UMR6634, University of Rouen, BP12, 76801 Saint-Etienne du Rouvray Cedex, France

<sup>b</sup> Ames Laboratory, Iowa State University, Ames, IA 50014, USA

<sup>c</sup> Oak Ridge National Laboratory, P. O. Box 2008, Oak Ridge, TN 37831-6115, USA

### ARTICLE INFO

#### Article history:

Received 24 August 2012

Received in revised form 20 September 2012

Available online 24 November 2012

#### JEL classification:

61.25.Mv

61.05.fm

#### Keywords:

Structure;

Al–Si;

Neutron diffraction;

Melt;

Superheat

### ABSTRACT

The structure of molten eutectic Al<sub>87.8</sub>Si<sub>12.2</sub> alloy has been studied by neutron diffraction during a temperature cycle. For comparison measurements were performed on pure molten Al. The measurements show that the alloy after heating above the liquidus contains particles of two kinds, aluminum-rich and silicon-rich. The silicon-rich particles are partly dissolved after a further heating. Earlier published data obtained by the  $\gamma$ -ray absorption technique of the density of the molten eutectic Al–Si alloy had demonstrated the existence of two temperatures above the liquidus temperature: A dissolution temperature  $T_d$ , at which the microstructure of the melt inherited from the ingot starts to dissolve and a branching temperature,  $T_b$ , at which the melt reaches a fully mixed state. The highest temperature that was possible to reach during the neutron experiments lies between  $T_d$  and  $T_b$ . The obtained results support these conclusions that molten alloys after melting are inhomogeneous up to a temperature well above the liquidus. Moreover, the difference in shape between the static structure factors measured by neutron and X-ray diffraction on molten aluminum is observed and is found to be more accentuated and to extend to larger wavevectors than in earlier works.

© 2012 Elsevier B.V. All rights reserved.

### 1. Introduction

The conditions in which melt solidification occurs greatly influence the structure, microstructure and properties of the resulting sample. To achieve the control of the properties of specimen through the understanding of the influence of the various synthesis conditions has been the aim of numerous studies in all fields of materials research. In particular, the effect of superheating the melt before quench has been investigated on different types of materials such as metallic glass ribbons and bulks [1–10], Al-based alloys [11–13], Ti–Al alloys [14], magnesium alloys [15], Sn–Pb alloys [16], Ni-based superalloys [17,18], nanocomposites [19]. Different solidification rates have also been tried [20–24] as well as different mixing procedures [25–28]. However, the conclusions from these studies have mostly been drawn from investigation of the morphology, structure and properties of the solidified state, rarely from the precursor liquid phase itself. Thus the interpretations of the liquid state have often been indirect.

With specific regard to Al–Si alloys, there exist a large bibliography on reported effect of superheat on the properties of the solidification product for standard alloys such as A356 [29,30] or A390 as well as binary alloys [31–34]. The reported effects are generally a finer and/or more uniform microstructure as well as an increase of yield strength, tensile strength and ductility in the samples produced with superheat

of the melt before solidification [35–37]. The structure for different compositions, including liquid Al [38–47] and at different temperatures as well as the effect of the addition of small amounts of a third element have been extensively investigated on an atomic scale by neutron and X-ray diffraction techniques or microscopy [48–55 and references therein,56–58].

However, from all these studies it is not possible to obtain a clear description of the structure as well as of the physical properties because the presented results differ substantially. Even a fundamental quantity in a diffraction experiment such as the height of the main peak of the static structure factor differs significantly between different published results as can be seen in Table 1 in which some selected results are listed. In this connection it should be emphasized that, as was first stressed in [59], static structure factors measured by neutron and by X-ray techniques are not expected to be identical because of the different scattering mechanisms in the two cases. This fact is experimentally verified by the values in Table 1.

The disparity between published results is also true for another fundamental quantity as the density. Thus, in three recent performed investigations of this quantity utilizing different experimental techniques (attenuation of  $\gamma$ -rays [60], the sessile drop method [61], and the Archimedian method [62]), the quoted densities for molten eutectic Al–Si alloy at 973 K differ by about  $\pm 1\%$ . In view of the achievable accuracy of the three techniques this may not be surprising but for an adequate comparison to calculated physical properties it might not be good enough. However, the discrepancy between the different results

\* Corresponding author. Tel.: +33 232955336.

E-mail address: [monique.calvo-dahlborg@univ-rouen.fr](mailto:monique.calvo-dahlborg@univ-rouen.fr) (M. Calvo-Dahlborg).

**Table 1**

Position and height of the main peak of the structure factor  $S(Q)$  for molten Al as reported in various publications. ND denotes neutron diffraction and XD X-ray diffraction.

Reference	Technique	Temperature (K)	Position of main peak ( $\text{\AA}^{-1}$ )	Height of main peak
Iqbal et al. [38]	ND	936	2.68	2.44
Mudry et al. [39]	XD	938	2.70	2.47
Takeda et al. [40,41]	ND	943	2.68	2.43
Waseda [42]	XD	943	2.71	2.48
Larsson et al. [43]	ND	950	2.70	2.20
Gabathuler et al. [44]	ND	953	2.70	2.25
Becker et al. [45]	XD	973	2.67	2.36
Roik et al. [46]	XD	973	2.68	2.12
Present work	ND	973	2.68	2.26
Stallard et al. [47]	ND	976	2.67	2.17
Jovic et al. [56]	ND	980	2.69	2.21

of measurements of the same physical properties and also their anomalous temperature dependences can in many cases be interpreted in terms of the structural inhomogeneities present after melting in the molten alloy and their dissolution when the liquid is heated further [50,63–65 and references therein]. The dissolution starts at a temperature  $T_d$  and at a branching temperature  $T_b$  well above the liquidus all inhomogeneities are dissolved. Some physical properties are thus different in heating and cooling modes. This is exemplified in Fig. 1 where density measurements taken from [11,60] for the eutectic molten Al–Si alloy during heating and cooling are presented. The difference between the heating and cooling data in the solid state ( $T < 850$  K) is due to the fact that the ingot did not completely fill the BeO container and also to the slow disappearance of the oxide layer with increasing temperature. The existence of a branching temperature at about 1560 K is clearly seen in Fig. 1 and indicated by the arrow. The phase diagram for the Al–Si system is a simple eutectic. In the solid phase the solubility of Si in Al is low, about 1.6 at%, while a considerable increase in solubility has been observed under high pressure [66] and by rapid quenching [20]. The results in Fig. 1 suggest that there exist thermodynamically stable phases in the molten state and that the relative amount of these phases also vary with alloy composition [63,65,67,68]. Similar anomalous behaviors have been observed in viscosity [69–72], resistivity [72–74], ultrasound velocity [70] and internal friction [21] measurements for many molten alloys.

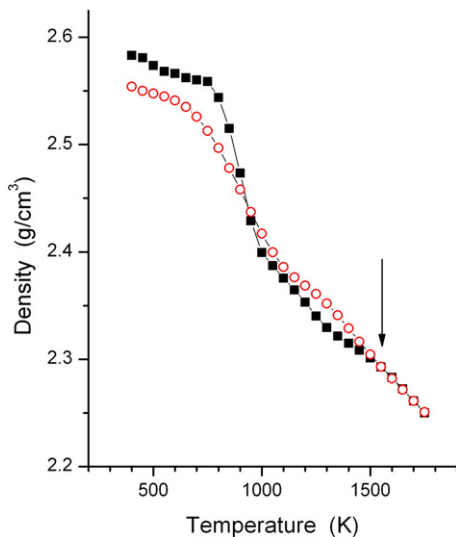


**Fig. 1.** The density of the eutectic  $\text{Al}_{87.8}\text{Si}_{12.2}$  alloy measured during heating (full squares) and subsequent cooling (empty circles). The arrow indicates the estimated branching temperature  $T_b$ .

However, the value of both the dissolution and branching temperatures is not sharp and it depends sensitively on the presence of very small amounts of impurities [11,63]. A strong support on atomic level for this picture has been obtained from small angle neutron scattering measurements [64,65]. *Ab initio* molecular dynamics simulations have also been carried out on the Al–Si system [75–77]. The number of atoms in some simulations is small (about 50 to 200) and for dilute systems they suffer significantly from bad statistics [78]. However, recent increases in computational efficiency simulations have enabled to include 500 atoms in a study of the eutectic Al–Si alloy [77]. Nevertheless, the comparison to accurate experimental data is essential for their validation. The alloy compositions as well as the alloy temperatures are not always the same in simulations and experiments and detailed comparisons are accordingly often difficult to make. Another complicating factor in such comparisons is the considerable difference between experimentally determined static structure factors.

One of the aims of the present work is to add to the clarification of the reason for the above-mentioned variation of the physical properties. Thus, experimental results on the structure on an atomic scale of the molten eutectic Al–Si alloy obtained by the neutron diffraction technique, obtained during heating and cooling are presented and discussed. In order to demonstrate the accuracy needed to obtain the desired information the adopted data correction procedure is discussed in detail. A preliminary interpretation of some of the data presented below has been earlier briefly published [79] and the microstructure, i.e. the structure on a length scale larger than about 1 nm, is discussed in another paper [65].

## 2. Theoretical background

The measured intensity in a diffraction experiment on a disordered material is proportional to the total static structure factor  $S(Q)$  that for a binary system in the Faber–Ziman formalism is given by

$$S(Q) = \frac{\left\{ I_a^{\text{coh}}(Q) - \left[ \langle b^2 \rangle - \langle b^2 \rangle^2 \right] \right\}}{\langle b^2 \rangle} \quad (1)$$

$$= \sum_{\alpha} \sum_{\beta} c_{\alpha} c_{\beta} b_{\alpha} b_{\beta} S_{\alpha\beta}(Q) / \langle b^2 \rangle$$

$I_a^{\text{coh}}(Q)$  is the intensity per atom of coherently scattered neutrons and  $c_i$  and  $b_i$  are the concentration and scattering amplitude of atoms  $\alpha$  and  $\beta$ , respectively.  $\langle b^2 \rangle$  is equal to  $c_{\alpha} b_{\alpha} + c_{\beta} b_{\beta}$  and  $\langle b^2 \rangle^2$  to  $c_{\alpha} b_{\alpha}^2 + c_{\beta} b_{\beta}^2$ .  $S_{\alpha\beta}(Q)$  is the partial structure factors.  $Q$  is the neutron wavevector transfer in the scattering process and it is given by  $Q = 2k \sin(2\theta)$  where  $k$  is the neutron wavevector and  $2\theta$  is the scattering angle. From the definition it follows that  $S(Q)$  is equal to one at large  $Q$ . The scattering amplitudes for Al and Si are 3.45 and 4.15 fm and thus the relative weight factors in Eq. (1) for the homogeneous eutectic Al–Si alloy are 0.64, 0.32 and 0.04, for  $S_{\text{AlAl}}(Q)$ ,  $S_{\text{AlSi}}(Q)$  and  $S_{\text{SiSi}}(Q)$ , respectively.

The static structure factor  $S(Q)$  is defined as the zero energy moment of the dynamic scattering function  $S(Q, E)$ . Accordingly,  $S(Q)$  is defined for a specific  $Q$  value as

$$S(Q) = \int_{Q=\text{const.}}^{+\infty} S(Q, E) dE \quad (2)$$

## 3. Experimental details

The neutron diffraction experiments were performed on the D4C diffractometer at the Institute Laue-Langevin, Grenoble, France [80]. The wavelength of the incident neutrons was 0.703  $\text{\AA}$  and accordingly the corresponding  $Q$  range was  $0.4 < Q < 16.5 \text{\AA}^{-1}$ . The Al–Si sample

Download English Version:

<https://daneshyari.com/en/article/7903995>

Download Persian Version:

<https://daneshyari.com/article/7903995>

[Daneshyari.com](https://daneshyari.com)